AIAA-93-3414-CP

Performance Results from a Test of an S-76 Rotor in the NASA Ames 80- by 120- Foot Wind Tunnel

Patrick M. Shinoda*

Aeroflightdynamics Directorate
U.S. Army Aviation RD&E Center - ATCOM
and
NASA Ames Research Center, Moffett Field, California

Wayne Johnson**

Johnson Aeronautics
Palo Alto, California

Abstract

A full-scale helicopter rotor test was conducted in the NASA Ames 80- by 120-Foot Wind Tunnel with a four-bladed S-76 rotor system. This wind tunnel test generated a unique and extensive data base covering a wide range of rotor shaft angles-of-attack and thrust conditions from 0 to 100 kt. Hover rotor performance data were compared with calculations based on momentum theory and previously acquired data from other test facilities to evaluate the capabilities of this wind tunnel as a hover facility. Forward flight rotor performance data were compared with the calculations from a comprehensive rotorcraft analysis, CAMRAD/JA, to evaluate the analytical modelling in the 0 to 100 kt speed range. Rotor performance data were also compared with previously acquired S-76 full-scale data from a test in the Ames 40- by 80-Foot Wind Tunnel to evaluate similarities and differences between the two facilities. Hover performance data show significant variations depending on the test configuration. Comparisons with theoretical predictions and other test data suggest that hover testing at an outdoor facility in absence of ground effect is required to make a final determination of the absolute accuracy of the hover data acquired in the 80 x 120. CAMRAD/JA calculations show good correlation with propulsive force data and a consistent level of overestimation of rotor power throughout the thrust and rotor shaft angle-of-attack envelope for a velocity range of 40 to 100 kt; below 40 kt, CAMRAD/JA power calculations diverge from the data. A comparison of the 80 x 120 data with data from a previous 40 x 80 wind tunnel test for 60 to 100 kt velocity range shows good correlation with rotor power and propulsive force data, except at the higher rotor shaft angles where there are some differences in rotor power. Results from the two S-76 wind tunnel tests suggest that the wind tunnel wall corrections should not be used for rotors operating in a nominal thrust range with rotor diameters up to 55% of the wind tunnel test section width, for $\mu \geq 0.150$, in either the 40 x 80 or 80 x 120.

Nomenclature

A	=	rotor disk area, πR^2, ft^2
b	=	number of rotor blades
c	=	airfoil chord length, ft
C_{LR}/σ	=	rotor wind-axis lift coefficient divided by rotor solidity, positive up, $L_R/\rho(\Omega R)^2 S_R$
C_P	=	rotor power coefficient, $P/A\rho(\Omega R)^3$
C_P/σ	=	rotor power coefficient divided by rotor solidity, $P/\rho(\Omega R)^3 S_R$
C_S	=	speed of sound, ft/s

*Aerospace Engineer. Member AIAA.
**Member AIAA.

C_T = rotor thrust coefficient, perpendicular to tip-path-plane, positive up, $T/A\rho(\Omega R)^2$

C_T/σ = rotor thrust coefficient divided by rotor solidity, positive up, $T/\rho(\Omega R)^2 S_R$

C_{XR}/σ = rotor wind-axis propulsive coefficient divided by rotor solidity, positive forward, $-D_R/\rho(\Omega R)^2 S_R$

D_R = rotor wind-axis drag, positive downstream, lb

F_M = Figure of Merit, $C_T^{3/2}/C_P\sqrt{2}$

L_R = rotor wind-axis lift, positive up, lb

M_{TIP} = rotor tip Mach number, $\Omega R/C_S$

P = rotor shaft power, Torque * Ω, ft-lb/s

R = rotor radius, ft

S_R = rotor blade area, bcR, ft^2

T = rotor thrust, lb

V_∞ = free stream velocity, ft/s

α_s = rotor shaft angle, positive aft of vertical, deg

κ = rotor induced power divided by ideal (momentum theory) induced power, P_i/P_{Ideal}

μ = advance ratio, $V_\infty/\Omega R$

ρ = free-stream air density, $lb\text{-}s^2/ft^4$

σ = rotor solidity, $bc/\pi R$

ψ = model yaw angle, clockwise relative to tunnel centerline, deg

Ω = rotor rotational speed, rad/s

Introduction

Wind tunnel testing has been extensively used in the development and improvement of rotorcraft designs, in addition to providing a data base for refinement of theoretical predictions. However, none of these tests, small-scale and specifically full-scale, have provided the necessary data in the low speed flight regime (below 60 kt) to validate prediction codes.

The Sikorsky Aircraft S-76 is one of the more thoroughly tested rotor systems, having undergone small-scale and full-scale wind tunnel testing in addition to flight testing. A full-scale test of the S-76 rotor system in the NASA Ames 40- by 80-Foot Wind Tunnel was performed and documented during the developmental phase of the rotor system.[1] There also have been flight test data, small-scale data, and full-scale hover data acquired with this rotor system at the Sikorsky Whirlstand Hover Facility and NASA Ames 40- by 80-Foot Wind Tunnel .[2] In all these tests, however, no data have been acquired in the speed range above 0 kt but below 60 kt.

To expand the existing S-76 data base and to investigate rotor performance and loads in the low speed (0 - 60 kt) flight regime, a full-scale S-76 rotor test was conducted at the NASA Ames 80- by 120-Foot Wind Tunnel. This wind tunnel test established a data base of rotor performance and loads for the 0 - 100 kt velocity range at various shaft angles and thrust conditions.

The wind tunnel test had multiple objectives, however, only some are discussed in this paper. The objectives discussed are (1) evaluating the capability of the 80 x 120 test section as a hover facility; (2) acquiring forward flight rotor performance data for comparison with analytical results; (3) acquiring S-76 forward flight rotor performance data in the 80 x120 wind tunnel to compare with existing[1] and future 40 x 80 data for evaluation of differences and similarities between the two full-scale wind tunnel facilities.

Additional test objectives not discussed in this paper are (1) evaluating rotor inflow and wake effects (varied by varying tunnel speed, shaft angle, and thrust condition) on wind tunnel test section wall and floor pressures; (2) establishing the criteria for the definition of flow breakdown (point where wall corrections are no longer valid) for this given size rotor and wind tunnel cross-sectional area; (3) evaluating the wide-field shadowgraph technique for visualizing full-scale rotor wakes[4]; and (4) evaluating the acoustic capability of the 80 x 120 for acquiring blade vortex interaction (BVI) noise in the low speed range and comparing BVI noise with in-flight test data.[5]

This paper presents a brief description of the experiment, description of the previous full-scale tests, and a description of the analytical model used. Hover and forward flight rotor performance results are discussed and compared with data from previous full-scale tests and

analytical calculations. Finally, conclusions of the research results are presented.

Description of the Experiment

NASA Ames 80- by 120-Foot Wind Tunnel

The 80- by 120-Foot Wind Tunnel is part of the National Full-Scale Aerodynamics Complex (NFAC) located at the NASA Ames Research Center. The tunnel has an open circuit with a closed, rectangular test section. The maximum test section flow speed is approximately 100 kt. Figure 1 shows a schematic of the wind tunnel circuit. The 80- by 120-Foot Wind Tunnel shares a portion of the flow circuit with the 40- by 80-Foot Wind Tunnel; both tunnels share a single drive system. The drive system consists of six fans rated at 135,000 maximum combined horsepower (101 MW). When operating in the 80 x 120 mode, a system of vanes and louvers are positioned so that the 40 x 80 circuit is closed off and the 80 x 120 leg forms a through-flow wind tunnel (Fig. 1). The drive fans pull outside air in through the 80 x 120 inlet and exhaust the air back to the atmosphere through louvers in the tunnel wall downstream of the tunnel fan drive system.

The test section is 80-ft high, 120-ft wide, and 193-ft long. The east wall of the test section has two doors that provide an access opening of approximately 80 ft in height by 120 ft in width. This opening provides room for the tunnel crane to move into the test section for installation of various size wind tunnel models.

General Hardware

The experiment was conducted in the 80- by 120-Foot Wind Tunnel using a production Sikorsky Aircraft S-76 rotor system. The rotor was mounted on NASA's modified Rotor Test Apparatus (RTA). Figure 2 shows the model installed in the wind tunnel. The Sikorsky Aircraft S-76 rotor system is four-bladed with coincident flap and lag articulation provided at the blade root by elastomeric bearings. Blade pitch is also permitted by the same bearing through the rotor spindle. Table 1 lists the S-76 main rotor parameters. The rotor system, including the hub, spindles, blades, and swashplate, is identical to the production model.

The RTA is a special-purpose test stand for operating helicopter rotors in the NFAC. The test stand was originally built in the mid-1970's. The RTA houses two-electric drive motors, a right-angle transmission, a new rotor balance with 22,000 lb thrust capability (installed in 1992) along with a primary and dynamic control system. The primary control system consists of three electro-hydraulic servo-actuators with an on-board hydraulic system with accumulators. The dynamic control system is integrated into the primary control system and provides time varying perturbation capability to the non-rotating swashplate.The RTA was first built as a symmetrical body of revolution that was 33.3 ft in length with a maximum diameter of 5.83 ft. In 1991, the RTA was modified to incorporate a fairing on top to enclose the raised rotor control system and the new balance. The new fairing on top of the RTA is 15.96 ft in length and has a maximum cross-section (3.5-ft wide by 4-ft tall) located near the rotor shaft.

The RTA was mounted in the wind tunnel on a three-strut (two main struts and one tail strut) support system placing the rotor hub nominally one rotor diameter above the wind tunnel floor. The model angle-of-attack was varied by changing the height of the gimballed tail strut. Rotor collective and cyclic pitch controls were inputted through the swashplate by means of three electromechanical/hydraulic actuators. All data presented in this paper were acquired with the first harmonic flapping trimmed to near zero.

Instrumentation

The new RTA rotor balance provides increased accuracy in measuring rotor hub loads. This five-component rotor balance measures rotor lift, drag and side forces, together with the rotor pitching and rolling moments. Also incorporated was an instrumented flex coupling to measure rotor torque. Both rotor balance and flex coupling were designed to measure static and dynamic loads. Table 2 lists the general capabilities and static load accuracies of the rotor balance.

Test Conditions and Envelope

There were three basic test conditions that were investigated. These were hover, tunnel speed sweeps at specific thrusts and rotor shaft angles-of-attack, and thrust sweeps at specific tunnel speeds and rotor shaft angles-of attack. The full range of test conditions is shown in Tables 3-5. Since the 80 x 120 is an open circuit wind tunnel, there are possible effects due to ambient outside wind speed and directions that can affect the tunnel test section conditions. To alleviate this concern, the majority of hover and low speed testing was performed when the ambient outside wind speeds were less than 5 kt and the air speed through the test section was less than 4 kt (based on tunnel dynamic pressure measurements).

Previous Test Data

As mentioned earlier, a full-scale 40 x 80 wind tunnel test of the S-76 rotor system was performed and documented during the rotor system developmental phase in 1977. Both hover and forward flight data were acquired during this program. Hover testing was done with tunnel overhead clamshell doors fully open with the shaft axis tilted 10 deg forward; the shaft was tilted to reduce rotor recirculation effects and ground effects. Systematic testing of tip shapes was conducted throughout the program; comparison studies for this paper are based on the production swept-tapered tip blade. There was no rotor balance during the 1977 test, so all of the rotor forces and moments were measured by the tunnel scale system; rotor torque was measured by instrumentation on the rotor shaft.

A full-scale hover test during this same time period took place at the Sikorsky Whirlstand Hover Facility.[2] The hover performance data from the whirlstand test were reduced by three percent in order to correct for test stand interference and ground effects.

Description of Analytical Model

Rotor performance calculations were performed using the comprehensive rotorcraft analysis CAMRAD/JA.[3] This comprehensive analytical model is designed to calculate rotor performance, structural loads, aircraft vibration and gust response, flight dynamics and handling qualities, and system aeroelastic stability.

The rotor structural model in CAMRAD/JA is based on engineering beam theory for a rotating wing with large pitch and twist. A single load path is assumed and the blade is considered to have a straight, undeformed elastic axis. The blade motion is described by rotating, free vibration modes, equivalent to a Galerkin analysis. For the present calculations, the rotor model had six coupled flap-lag modes (including rigid flap and lag motions), together with rigid pitch motion (from control-system flexibility) and one elastic torsion mode. Calculations were performed using a 15 deg azimuth increment, with 12 harmonics of all blade structural degrees of freedom.

The rotor aerodynamic model in CAMRAD/JA is based on second-order lifting-line theory, and uses steady two-dimensional airfoil characteristics (tables of section lift, drag, and pitching moment, defined as a function of angle-of-attack and Mach number) with a vortex wake. The airfoil characteristics of the S-76 rotor blades were obtained from Sikorsky Aircraft. The aerodynamic model includes static stall, a yawed-flow and swept-blade correction, and unsteady aerodynamic forces from thin airfoil theory. For the swept tip, allowance is also made for offsets of both the aerodynamic center and the center of gravity from the blade reference axis.

There are three levels of wake model in CAMRAD/JA. These are uniform inflow (used for hover in this paper), nonuniform inflow with a prescribed wake geometry, and nonuniform inflow with a free wake geometry (used for the majority of forward flight comparison studies in this paper). Uniform inflow here refers to an empirical model based on momentum theory. Nonuniform inflow calculates the induced velocity at the rotor blade from a vortex wake model. A key parameter governing the effects of the wake on the rotor airloading is the radius of the tip vortex viscous core. A core radius of 20 percent chord was used, based on airloads correlations for other rotors.

The trim solution was obtained for a specified tunnel speed, rotor shaft angle-of-attack, and atmospheric conditions. The trim iteration adjusted the rotor controls to attain the specified thrust and zero tip-path-plane tilt relative to the shaft.

Results and Discussion

In the following sections, results are provided for hover and forward flight conditions.

Hover performance measurements are compared with momentum theory calculations and previously acquired full-scale measurements. The validity of using the 80 x 120 as a hover facility is discussed.

Forward flight performance measurements are presented for speed and thrust sweeps. The data are compared with CAMRAD/JA calculations (using different wake models); limitations of the analysis in computing low-speed rotor performance are discussed. The data are also compared with the 40 x 80 data set to investigate facility and wall effects.

Hover Performance

The purpose of the hover testing was to evaluate the capability of the 80 x 120 as a hover facility. If proven as a viable hover facility, the 80 x 120 provides test section dimensional advantages over other wind tunnels in addition to environmental advantages over outdoor facilities.

The approach was to test the rotor for two basic configurations as shown in Figs .3 to 4. The first configuration was with the model aligned with the tunnel centerline and facing the tunnel inlet. In this configuration, effects of shaft angle on rotor power at given thrust conditions were investigated by conducting thrust sweeps at several shaft angles. In-ground effect conditions were defined by identifying noticeable effects of shaft angle on rotor power at a given thrust. If an in-ground effect condition was identified, the next step was to determine the shaft angle required to maximize rotor power for a given thrust, thus minimizing or eliminating the ground effect. The shaft angle selected was 15 deg and was used for the second configuration; the reason for this selection will be discussed later. The second configuration was with the model yawed 90 deg clockwise, placing the model nose facing the main tunnel access doors (east wall). This placed the rotor shaft centerline approximately 73 ft from the west wall. With the tunnel doors (east wall) in the open position and the rotor shaft angle set to 15 deg, this provided approximately an 80-ft high by 120-ft wide opening for the rotor wake to exit the facility. The purpose of this configuration was to determine if the elimination of one of the tunnel walls would reduce facility effects in hover. These data are presented in Figs. 5-11.

Momentum theory calculations, performed using CAMRAD/JA, are presented in Figs. 5-7 and 9-11. They are included to help assess configuration effects on the hover performance measurements. In these calculations, the wake-induced velocity (uniform over the rotor disk) is equal to the ideal momentum theory value times an input factor κ (always greater than 1.0). This factor κ is the ratio of the induced power to ideal power. Because of the non-ideal induced power losses, κ typically has been a value of about 1.15 for full-scale rotors in hover.[6] Note that calculated total hover power is equal to κ times the ideal induced power plus profile power. Calculated and measured power at low thrust levels are in good agreement, as shown in Fig. 5. This suggests the profile power is being calculated correctly and this also indicates the airfoil tables are correct. Otherwise, a blade drag increment would be required to achieve a match of calculated and measured power at low thrust. In this instance, the calculated power matched the experimental data, therefore requiring no such corrections. Once the profile power has been verified, momentum theory calculations using various values of κ can be compared with the measured performance at moderate and high thrust; this provides a means of determining the value of κ implied by the test data. A value of κ below 1.10 or above 1.20 could imply significant effects of the wind tunnel walls, ceiling, and floor. A significantly lower value of κ would be considered in-ground effect. The limitation of this approach is the assumption that the profile power is being calculated correctly at moderate and high thrust, as well as at low thrust. Errors in the calculation of profile power may exist because of the assumption of uniform inflow (so the radial distribution of the blade angle-of-attack is not correct), or because errors in the blade drag increase with angle-of-attack (in the airfoil tables).

Figure 5 compares S-76 rotor hover performance for two different model yaw angles (ψ = 0 deg includes all shaft angles and ψ = 90 deg at 15 deg shaft angle) together with predictions based on momentum theory. To assess the trends and scatter in the data, Fig. 6 shows the same data in terms of figure of merit. For ψ = 0 deg, the power is higher (Fig. 5) and the figure of merit is lower (Fig. 6) when compared to the ψ =90 deg configuration. This figure of merit difference (Fig. 6) increases as the thrust is increased. The higher figure of merit requirement for ψ = 90 deg suggests that the rotor is experiencing an in-ground effect condition. This is also indicated by momentum theory, which shows a κ value less than 1.10, a value less than real helicopter rotors. A ground effect correction[7] was applied to this data to determine if the performance would be more representative of κ = 1.15; for this correction, a rotor height-to-diameter ratio of 1.027 was used. Figure 7 shows that with the ground effect correction, the data shifts closer to the nominal κ=1.15 value but not enough to account for the higher figure of merit. The majority of this difference appears to be due to some type of facility effect.

The data in Fig. 6 includes all shaft angles tested at ψ = 0 deg. These data match well with the κ value of 1.15 at the low thrusts but then diverges to a κ value greater than 1.20 at higher thrusts. The data also shows an increase in data scatter as rotor thrust is increased, which the following discussion shows is partly caused by rotor shaft angle-of-attack sensitivity.

To determine the possible effects of shaft angle on hover performance for ψ = 0 deg, Figs. 8-10 were generated. Figure 8 shows the effects of shaft angle on rotor figure of merit at two thrust conditions: C_T/σ =0.08 and 0.10. Even with significant scatter, the data indicates that power increases and figure of merit decreases as rotor shaft angle is decreased from 15 to -5 deg. However, power differences between -10 deg and -15 deg could be considered within test repeatability. This was true for all thrust conditions tested at these two shaft angles. To further examine the effect of shaft angle, Fig. 9 shows a comparison of figure of merit for two extreme shaft angles (the data show some scatter, so curve fits are presented in Fig. 9). This plot verifies what Fig. 8

indicates - that the figure of merit is influenced by shaft angle. Based on this comparison, the best data (in terms of being closest to $\kappa = 1.15$) is at +15 deg shaft angle. Even at the highest thrust at this shaft angle, however,the figure of merit is still lower than expected (based on momentum theory calculations). Notice in Fig. 9 that the shaft angle of 15 deg matches closer to the calculations with $\kappa = 1.20$ at higher thrusts. Thus, there are facility effects for $\psi = 0$ deg (not ground effect, which would cause the figure of merit to be higher than expected). A possible facility effect is that the rotor is pumping air through the wind tunnel circuit , basically acting as a pump in a large open-ended duct, therefore requiring more power as compared to operating in free air.

Figure 10 shows there is considerable more data scatter at positive shaft angles (α_S= 10 deg and 15 deg) than the negative shaft angles (α_S= -5 deg, -10 deg and -15 deg). With further detailed comparisons between data acquired at shaft angles of α_S= -5 deg, -10 deg and -15 deg, data for -15 deg shaft angle was determined to be the best hover data in terms of least amount of data scatter. Confirmation was again made that there was no significant change in rotor performance between -10 deg and -15 deg shaft angle. There are a number of possibilities for this scatter at shaft angles greater than -5 deg. One possible cause may be the inflow characteristics to the rotor. When the rotor is positioned at α_S= 10 deg or 15 deg, the flow of air is drawn into the rotor from the exhaust section of the tunnel, through the greatly reduced area at the tunnel drive system section, through tunnel guide vanes, through a 30 deg turn into the six large turning vanes, and then through the test section area into the rotor. The air drawn into the rotor from this direction is probably nonuniform; in addition, there is possibly air being drawn in from the tunnel inlet. Another possibility or contributing influence to the scatter of the data is rotor wake recirculation causing high level, low frequency unsteadiness resulting in significant scatter in the steady-state data; the level of recirculation also appears to be sensitive to shaft angle. The final possibility and the most likely is that all are contributing to the data scatter for all shaft angles.

As a final comparison, Fig. 11 presents S-76 rotor hover performance data from earlier 40 x 80 and Sikorsky whirlstand tests, and the best hover data (in terms of scatter) from the 80 x 120 1992 test. The whirlstand data rises more steeply and begins to level off at a higher figure of merit than the other data sets and momentum theory calculation for $\kappa = 1.15$. Good correlation exists between the 40 x 80 and 80 x 120 data for $C_T/\sigma \leq 0.04$. However, from C_T/σ= 0.04 - 0.09 the 40 x 80 data diverges from the 80 x 120 data showing better rotor performance and then converges with the whirl tower results. The 40 x 80 and whirl tower results appear more reasonable based on the momentum theory calculations. However, the whirl tower measurements included a significant ground effect and blockage effect correction (the whirl tower results in Fig. 11 include a 3 percent correction to measured power). The 40 x 80 measurements were made with the rotor only one-half diameter above the tunnel floor. These variations in data from test to test show that each facility may have some type of an effect on rotor performance and this reinforces the requirement that outdoor hover testing out of ground effect must be performed to establish how, or if, the 80 x 120 hover data at -15 deg shaft angle should be corrected.

Speed Sweep Rotor Performance

One of the major objectives of this test was to compare theoretical calculations with test data, especially in the 0 - 60 kt speed range (referred to as "the backside of the power curve"). This was accomplished by performing speed sweeps at three specific thrust conditions (C_T/σ=0.065, 0.080, 0.100) for a range of rotor shaft angles from -10 deg to 10 deg. In the following section, these data are presented and compared with CAMRAD/JA's calculations.

The effects of rotor shaft angle and advance ratio on rotor power for fixed C_T/σ of 0.065, 0.080, and 0.100 are shown in Figs. 12, 13, and 14, respectively. Figure 12 shows there are distinctive power profiles for a given shaft angle as a function of advance ratio at a fixed C_T/σ of 0.065. At a shaft angle of -10 deg, the power decreases with decreasing advance ratio until μ=0.10 and then increases. For a shaft angle of 5 deg, the power always increases with a reduction in advance ratio. However, at a shaft angle of -2 deg, the power stays relatively constant until μ=0.10 and then increases. Figure 12 also shows that the differences in power requirements between shaft angles increases with advance ratio. This spread in power requirements widens even further with the increase in rotor thrust as shown in Figs. 13 to 14. The data also shows that the power requirement increases with decreasing shaft angle for any given advance ratio and thrust condition.

Also shown in Figs. 12-14 are CAMRAD/JA calculations using the free wake geometry. These figures show that CAMRAD/JA overestimates rotor power at a relatively consistent level for advance ratios of 0.10 to 0.25 at all shaft angles and all thrust conditions. This overestimation could be caused by a number of different factors. One possibility is that some parameters of the wake model are introducing a uniform increase in

calculated induced power. Another possibility is that one of the calculated power components (parasite, profile, or induced) needs to be improved. This latter possibility was investigated for this paper. Since the rotor propulsive force is well predicted at all shaft angles (shown later in this paper), the parasite power calculation is considered to be accurate. The insensitivity of the error to thrust and speed suggests that the induced power (which varies significantly with C_T and μ) is accurate (except at the lower speed and high thrust, as shown in Fig. 14). There remains the profile power, which for each thrust should be nearly constant over the speed range considered here. The nearly constant error of approximately $\Delta C_P/\sigma = 0.0005$ corresponds to about $\Delta c_d = 0.0040$ in mean blade drag coefficient. Subtracting this value from the drag in the airfoil table would not be appropriate at small angle-of-attack, however, since 0.0040 is a large drag increment and the hover calculations are good at low thrust. Possibly the drag in the airfoil tables at moderate angle-of-attack is too high.

The effects of rotor thrust and advance ratio on rotor power for a rotor shaft angle of -2 deg are compared with CAMRAD/JA calculations using two wake models (nonuniform inflow with prescribed wake geometry and nonuniform inflow with free wake geometry) in Fig. 15. The figure shows the nonuniform inflow with free wake calculations overestimate rotor power at a relatively consistent level over the test data for advance ratios of 0.10 to 0.25 at all thrust conditions. However, at the lower advance ratios, this calculation diverges from the test data. This indicates that the free wake modelling definitely needs to be improved at the low advance ratios. The prescribed wake calculations match the free wake calculations at an advance ratio of 0.25, but then slowly diverge to a lower value as the advance ratio is reduced to 0.10.

As stated in the previous paragraph, the free wake modelling (which has a significant effect on the calculation of induced power) needs to be improved at the low advance ratios. To further understand the effects of the prescribed wake and free wake calculations on the calculated induced power and to provide some direction toward what a realistic value of κ is at low advance ratios, Fig. 16 was generated. The figure shows the calculated ratio of induced to ideal power for the two wake models and a profile of what the κ ratio should be based on test data for C_T/σ of 0.080. The calculated values of κ for both methods generally decrease as advance ratio decreases. With the prescribed wake geometry, κ continues to decrease below the advance ratio of 0.15, and eventually becomes less than 1.0 (calculated induced power less than the minimum possible). The prescribed wake geometry places the wake too far from the rotor disk at low speeds, so the induced velocity is too small resulting in the lower power required than the free wake calculations as shown in Fig. 15. With the free wake geometry, κ has a relatively constant value from $\mu = 0.15$ to 0.10, and then increases as the advance ratio decreases to 0.05. The good correlation of calculated total power, as shown in Fig.15, means that the free wake model is accurate down to $\mu = 0.10$. But at lower speeds, the wake influence is exaggerated using either wake geometry of CAMRAD/JA. At hover, a κ value of 1.15 is expected.[6] To assess what the κ value or κ profile should be between an advance ratio of 0 to 0.15, the measured performance can be used. The induced power can be estimated by subtracting the parasite power (from measured speed and propulsive force) and profile power (assumed to be a constant value over a range of $\mu = 0.04$ to 0.15 for a fixed thrust), from the total measured power. The κ values based on induced power calculations from the measured total power values are then matched to the calculated κ for $\mu = 0.10$ to 0.15. The results are shown in Fig. 16. The value of κ can be expected to be relatively constant from $\mu = 0.15$ down to 0.07, then reducing to the hover value. Based on these results, both wake geometry calculations must be improved to obtain such behavior.

Thrust Sweep Rotor Performance

Facility effects are addressed in this section of the paper by comparing 80 x 120 rotor performance data with the 40 x 80 rotor performance data acquired in 1977. The data are presented for thrust sweeps at advance ratios ranging from 0.15 to 0.25 and shaft angles ranging from -15 deg to 10 deg. In addition, corrections for wall effects in the 40 x 80 are discussed. Finally, the 80 x 120 rotor performance data is compared with CAMRAD/JA calculations.

Full-Scale 80 x 120 and Full-Scale 40 x 80 Data Comparison

Results from these two full-scale tests are shown in Figs. 17 - 22. Neither set of data has wall corrections applied, and the 1977 data for α_S of -2 deg is interpolated data (data were interpolated from 0 deg and -2.5 deg or -5 deg data).

A comparison of rotor power vs rotor lift for various rotor shaft angles at advance ratios of 0.15, 0.20, and 0.25 for the two tests are shown in Figs. 17, 18, and 19, respectively. The data sets complement each other and correlate well with a few exceptions. Fig. 17 shows that for a shaft angle of -5 deg and an advance ratio of 0.15, the two data sets match each other. The 1977 data also

matches the 1992 data at the lower lift conditions at a shaft angle of -2 deg, but then a small divergence to a lower power requirement is shown as rotor lift is increased. At an advance ratio of 0.20 (Fig. 18), the 1977 data requires a slightly larger power requirement through the mid-range of rotor lift for a shaft angle of -2 deg whereas the 1977 data indicates a lower power requirement than the 1992 data throughout the rotor lift range for a shaft angle of 10 deg. For an advance ratio of 0.25 (Fig. 19), the two sets of test data correlate well for a shaft angle of -5 deg and -2 deg.

A comparison of rotor propulsive force vs rotor lift for the two tests for various rotor shaft angles at advance ratios of 0.15, 0.20, and 0.25 are shown in Figs. 20, 21, and 22, respectively. The two sets of data match very well, with the exception of the α_S = -2 data for μ = 0.20 (Fig. 21).

In general, the data from these two full-scale tests match relatively well despite the differences in facility size, rotor measurement systems, and model test stand shape. However, to clearly define the differences between the facilities, a test with the S-76 rotor system in the 40 x 80 matching the 80 x120 S-76 test matrix is recommended since the 1977 40 x 80 data set is sparse for the 0 - 100 kt speed range.

Full-Scale 40 x 80 Corrected and Uncorrected Data Comparison

Note that the data compared above have not been corrected in any way. In particular, the effect of the wind tunnel walls on the local angle-of-attack was not accounted for. To assess the effects of a typical wall correction method, the data from the 1977 test was analyzed both with and without wall corrections and compared with 1992 80 x 120 data. The correction method used was the conventional Prandtl-Glauert analysis where the rotor is considered a circular wing. The result is a correction to the angle-of-attack. This wind tunnel wall correction changes the rotor propulsive force, C_{XR}/σ. The power as a function of rotor lift at fixed shaft angle is not affected by the correction.

The effects of the angle-of-attack correction on the 1977 data for various rotor shaft angles and thrust on rotor propulsive force at advance ratios of 0.15,.0.20, and 0.25 are shown in Figs. 23, 24, and 25, respectively. Also shown for comparison is the uncorrected data from the 1992 test (note that wall corrections for this test will be smaller due to the relative large size of the 80 x 120 wind tunnel). The correction to the 1977 data at maximum lift of 15,000 lb is about 2.5 deg for an advance ratio of 0.15 and decreases to approximately 0.9 deg at an advance ratio of 0.25. The present method of correction does not appear to be effective at these advance ratios. On the contrary, the results from the 40 x 80 and 80 x 120 compare well without wall corrections in either case (Figs. 23-25). Therefore, the influence of the wind tunnel walls is small, and an angle-of-attack correction should not be used, for rotors with diameters up to 55 percent of the wind tunnel width, operating at normal thrust and advance ratios above 0.15, in either the 40 x 80 or 80 x 120.

Full-Scale 80 x 120 Data and CAMRAD/JA Calculations Comparison

CAMRAD/JA calculations have already been compared with S-76 1992 data, in Figs. 12-14, to determine the effects of advance ratio and shaft angle at specific thrust conditions on rotor power. The results showed that rotor power calculations overestimated at a consistent level for advance ratios of 0.10 to 0.25 for all shaft angles for three specific thrust conditions (C_T/σ of 0.065, 0.080, and 0.100). To further understand how well CAMRAD/JA calculations compare with measured data for a wider range of thrust conditions, a test matrix of thrust sweeps were conducted for various shaft angles and specific advance ratios. The advance ratios that will be discussed in this section are 0.15, 0.20, and 0.25.

Comparisons between measured rotor performance and CAMRAD/JA calculations using a free wake geometry are shown in Figs. 26-28. Figure 26 shows that there are distinctive power profiles for a given shaft angle as a function of lift at a fixed advance ratio of 0.15. At a shaft angle of -10 deg, power increases with increased lift at a higher rate compared to other shaft angles. For a shaft angle of +10 deg, power stays relatively constant at a low value until lift reaches C_{LR}/σ of 0.08 where power increases at a lower rate as compared to other shaft angles. Figure 26 also shows the differences in power requirements between various shaft angles increases with lift. This spread in power requirement widens even further with increase in advance ratio as shown in Figs. 27-28. The data also show that the power requirement increases with decreasing shaft angle for any given advance ratio and thrust condition. These figures confirm the results of Figs. 12-14: CAMRAD/JA overestimates rotor power at a relatively consistent level for all shaft angles and thrust conditions tested for advance ratios from 0.10 to 0.25.

The effects of rotor shaft angle and thrust sweep on rotor propulsive force for advance ratios of 0.15, 0.20, and 0.25 are shown in Figs. 29, 30, and 31, respectively. CAMRAD/JA calculations compare well with data for all

three advance ratios with only a few differences. In particular, CAMRAD/JA shows a small trend of increasingly underestimating the propulsive force as advance ratio is increased. This small variation may be due to small errors in sectional lift and drag coefficients used in the analysis or differences in inflow characteristics.

Conclusions

Rotor performance results from the S-76 test in the 80- by 120-Foot Wind Tunnel have been compared with calculations and other tests results. A high quality data set at low forward speeds has been obtained in the 80 x120, to support future rotor developments and theory improvements. The study has resulted in the following conclusions:

Hover performance is significantly affected by the configuration of the test installation, testing facility, and to a lesser degree by rotor shaft angle. Hover data with the least amount of scatter were obtained with ψ=0 deg at -15 deg shaft angle. Data at ψ=0 deg at 15 shaft angle more closely match momentum theory calculations of power with κ=1.15 (out-of-ground effect) than other test configurations; however, the differences between measured and calculated performance are thought to be due to facility effects. Ground effect corrections to data obtained at ψ=90 deg and 15 deg shaft angle were found to be small, accounting for only a small part of the discrepancy between measured and momentum theory calculations (using κ=1.15) of power. Thus, the remaining differences are thought to be caused by facility effects. Based on the discrepancies of measured rotor performance in the different facilities, in addition to comparisons with momentum theory calculations, hover testing at an outdoor facility in the absence of ground effect is recommended. Such a test is required to assess the quality of the hover data acquired to date, particularly the ψ=0 deg, -15 deg shaft angle 80 x 120 data.

CAMRAD/JA calculations using a free-wake geometry show good correlation with propulsive force data and a nearly consistent level of overestimation of rotor power throughout the thrust and shaft angle-of-attack range tested for μ=0.10-0.25. Below μ=0.10 both the free- and prescribed-wake geometry calculations diverge from the measured power.

Without wall corrections, the rotor power and propulsive force data from the 80 x 120 test matches relatively well with the limited data available from the 1977 40 x 80 test for μ=0.10-0.25, with some noticeable differences in rotor power at the higher shaft angles. Because the 40 x 80 data set is not as extensive in the low-speed range (0-100 kt) as the 80 x 120 data set, a test of the S-76 rotor in the 40 x 80 matching the 80 x 120 test matrix is recommended to clearly define differences between the two facilities.

Applying wall corrections to the 40 x 80 data did not improve the comparisons with the 80 x 120 data for $\mu \geq 0.15$. Therefore, for rotors with diameters up to 55% of the wind tunnel test section width and operating at a nominal thrust range with $\mu >= 0.15$, wall corrections are considered unnecessary in either facility.

Acknowledgments

We would like to acknowledge the significant efforts of the NASA test team in the conduct of this experimental investigation. The author would also like to thank Dr. Jane Leyland for generating preliminary performance predictions.

References

[1]Johnson, W., "Performance and Loads Data From a Wind Tunnel Test of a Full-Scale Rotor With Four Blade Tip Planforms," NASA TM 81229 / USAAVRADCOM TR80-A-9, September 1980.

[2]Jepson, D., Moffitt, R., Hilzinger, K., and Bissel, J., "Analysis and Correlation of Test Data From an Advanced Technology Rotor System," NASA CR 3714, August 1983.

[3]Johnson, W., "A Comprehensive Analytical Model of Rotorcraft Aerodynamics and Dynamics / Johnson Aeronautics Version," Johnson Aeronautics, Palo Alto, CA, 1988.

[4]Swanson, A., "Application of the Shadowgraph Flow Visualization Technique to a Full-Scale Helicopter in Hover and Forward Flight," AIAA Paper 93-3411, AIAA Eleventh Applied Aerodynamics Conference, Monterey, CA, August 1993.

[5]Yamauchi, G., Signor, D., Watts, M., Hernandez, F., and LeMasurier, P., "Flight Measurements of Blade-Vortex Interaction Noise Including Comparisons with Full-Scale Wind Tunnel Data," American Helicopter Society 49th Annual Forum, St. Louis, MO, May 1993.

[6]Johnson, W., *Helicopter Theory*, Princeton University Press, New Jersey, 1980.

[7]Cheeseman, I. and Bennett, W., "The Effect of the Ground on a Helicopter Rotor in Forward Flight," ARC R&M 3021, September 1955.

TABLE 1 Main Rotor Parameters

Parameter	Value	
Radius	22	ft
Nominal Chord	15.5	in
Solidity Ratio	.0748	
Number of Blades	4	
Airfoils	SC1095 and SC1095R8	
Flapping Hinge offset	3.70%	radius
Lock No.	11.6	
100% RPM	293	
100% tip speed	675	fps

TABLE 2 RTA Rotor Balance Calibration Accuracy

			Std. Deviation of Error		
Parameter	Maximum Capacity		Value		% Capacity
Normal Force	22,000	lb	25	lb	0.12
Side Force	4,400	lb	7	lb	0.16
Axial Force	4,400	lb	12	lb	0.27
Pitching Moment	694,000	in-lb	324	in-lb	0.05
Rolling Moment	694,000	in-lb	504	in-lb	0.07
Torque	36,083	ft-lb		--	--

TABLE 3 Hover Test Matrix

Shaft Angles, α_s	-15°, -10°, -5°, 0°, 5°, 10°, 15°*
C_T/σ	0.02 - 0.12
Tip Mach No.,M_{TIP}	0.605
ψ	0°, 90°*

*Note: For ψ=90°, hover data taken only at α_s=+15°

TABLE 4 Speed Sweep Test Matrix

V_∞ = 0-100 kt
M_{TIP}: 0.605 (675 fps)

α_s	THRUST, lb		
	8,000 (C_T/σ=.065)	9,850 (.080)	12,320 (.100)
10°		X	X
5°	X	X	X
0°		X	
-2°	X	X	X
-5°	X	X	
-10°	X	X	X

TABLE 5 Thrust Sweep Test Matrix

C_T/σ=0.03-0.125
M_{TIP}: 0.605 (675 fps)

VKTS	μ	α_s					
		10°	5°	0°	-2°	-10°	-15°
20	0.050				X		
32	0.080			X			
40	0.100	X	X		X	X	X
50	0.125	X	X				
60	0.150	X	X		X	X	X
80	0.200	X	X		X	X	
100	0.250	X	X		X	X	X

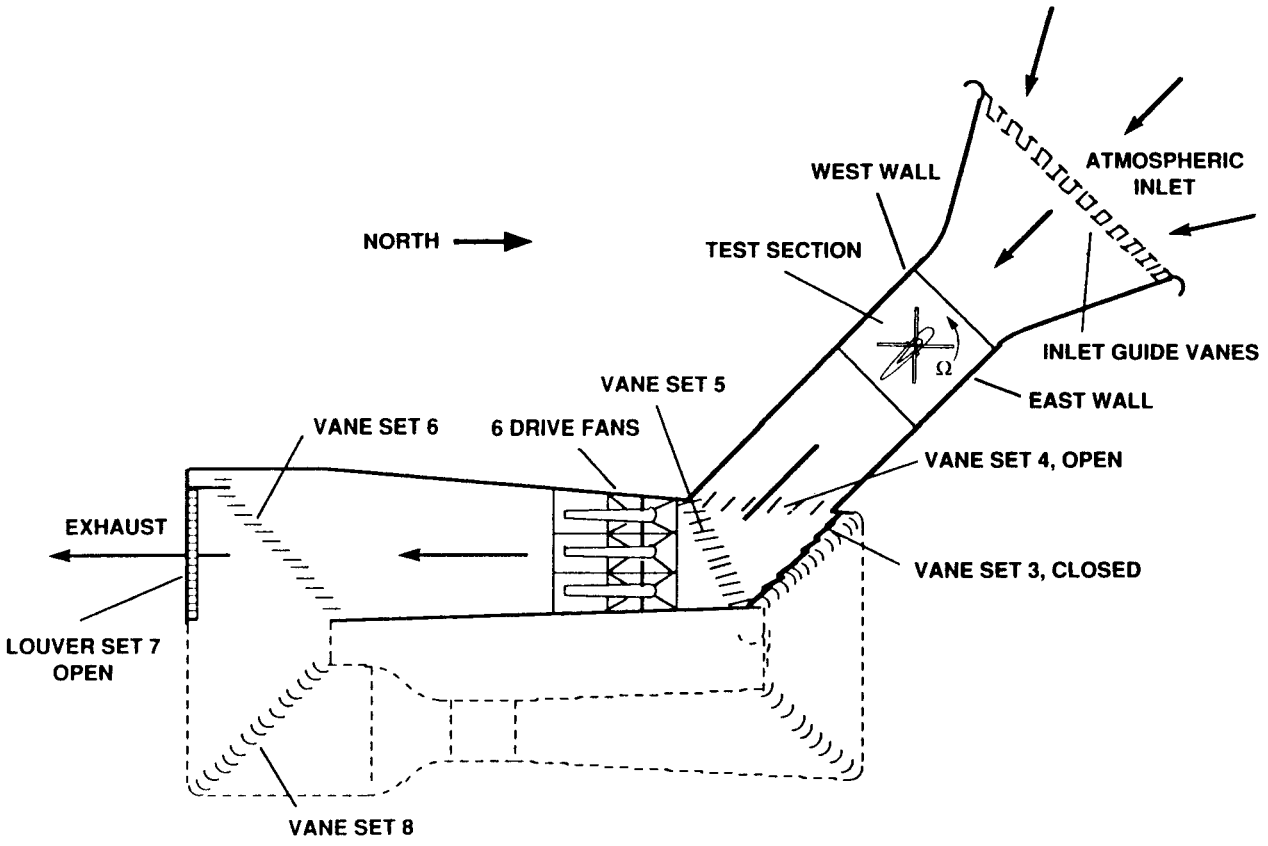

Fig. 1 80- by 120-Foot Wind Tunnel Ciruit.

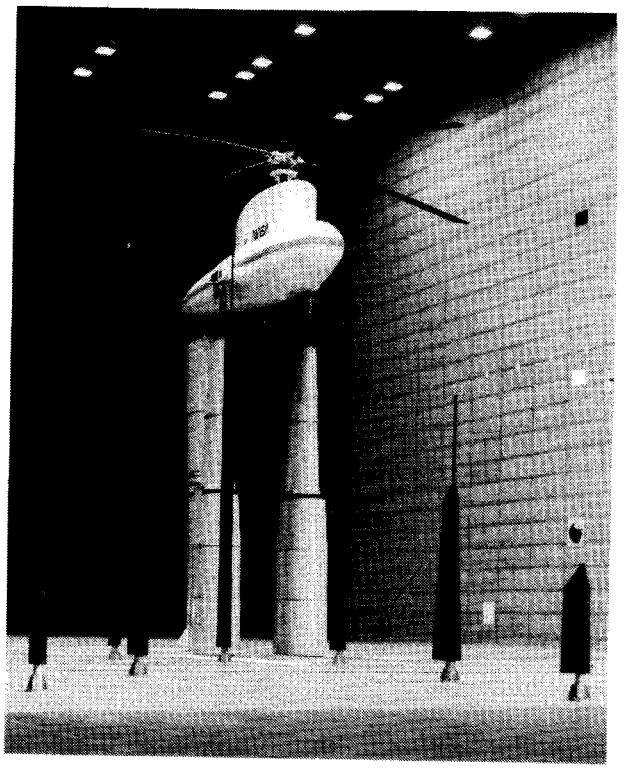

Fig. 2 S-76 Rotor System installed on Rotor Test Apparatus in the Ames 80- by 120-Foot Wind Tunnel.

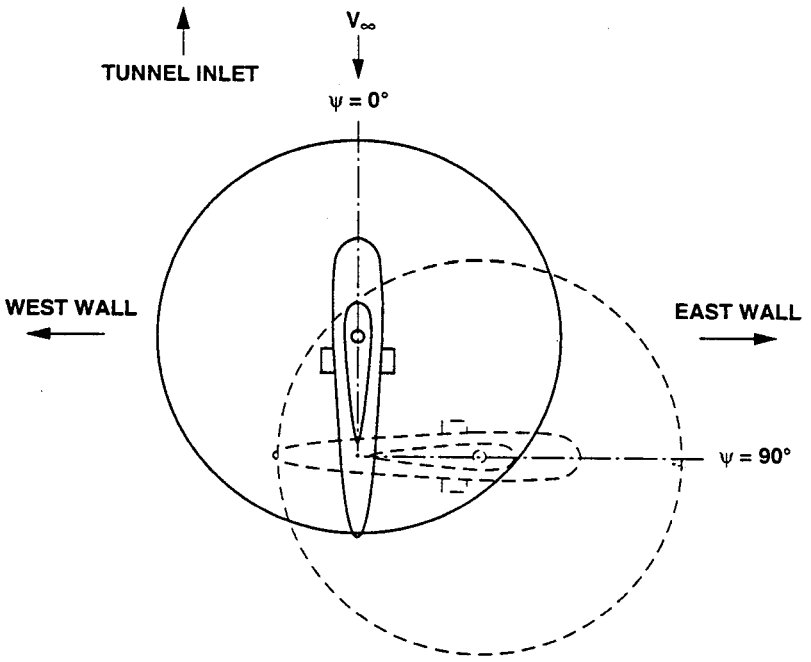

Fig. 3 Plan view of model in the 80 x 120 tunnel test section ψ= 0 deg and 90 deg

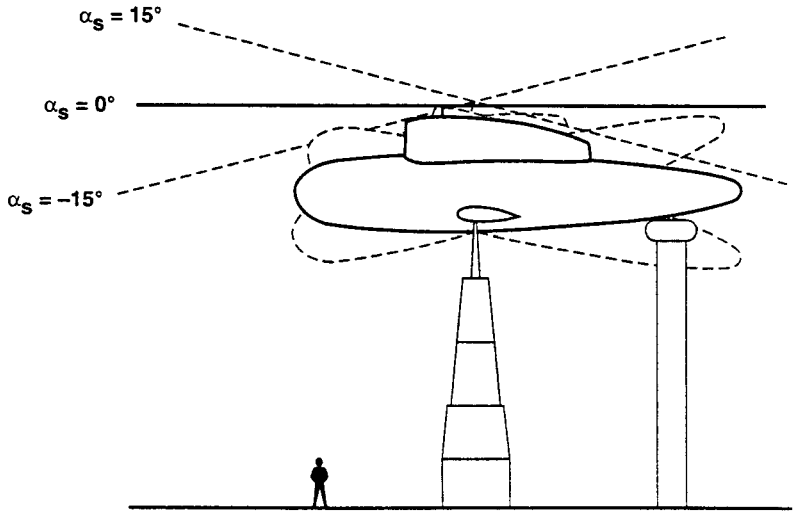

Fig. 4 Side view of model in tunnel test section α_s= 0 deg, -15 and 15 deg.

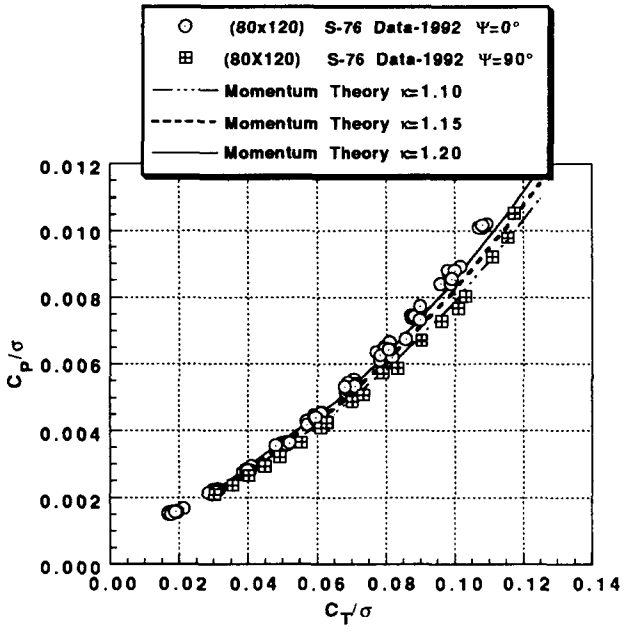

Fig. 5 Comparison of experimental rotor hover power at ψ= 0 deg and 90 deg with momentum theory, M_{TIP}=0.605

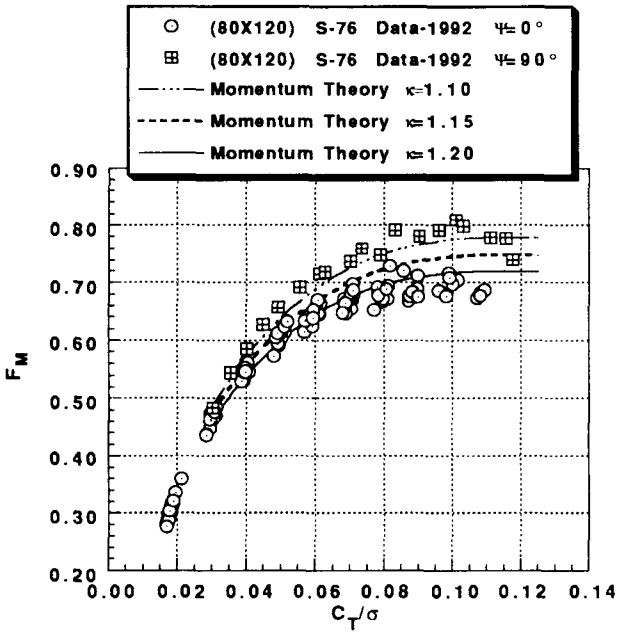

Fig. 6 Comparison of experimental rotor hover figure of merit at ψ= 0 deg and 90 deg with momentum theory predictions, M_{TIP}= 0.605.

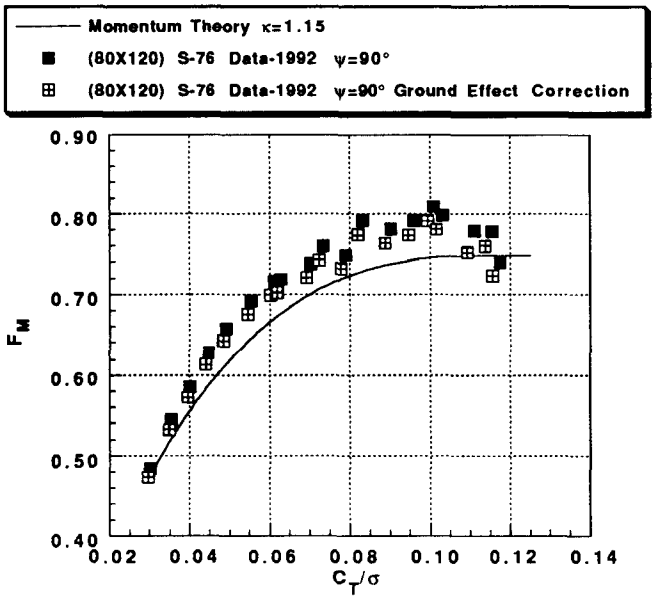

Fig. 7 Comparison of figure of merit with and without ground effect corrections for ψ= 90 deg, M_{TIP}= 0.605

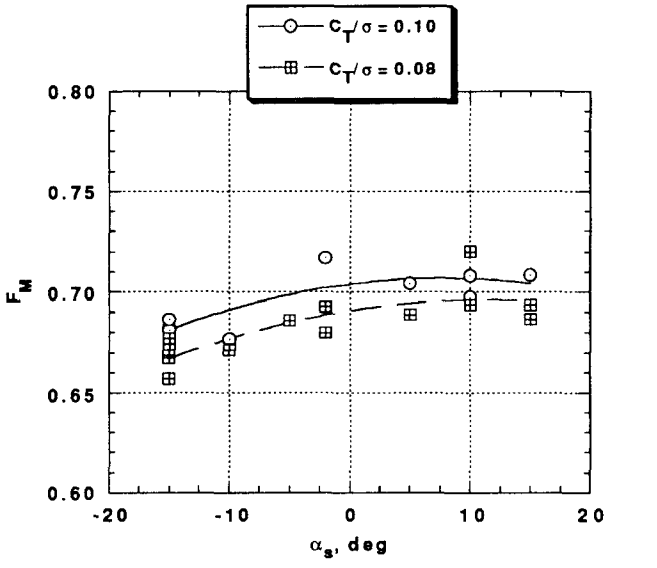

Fig. 8 Effect of rotor shaft angle sweep on figure of merit at C_T/σ= 0.08, 0.10, M_{TIP}= 0.605 .

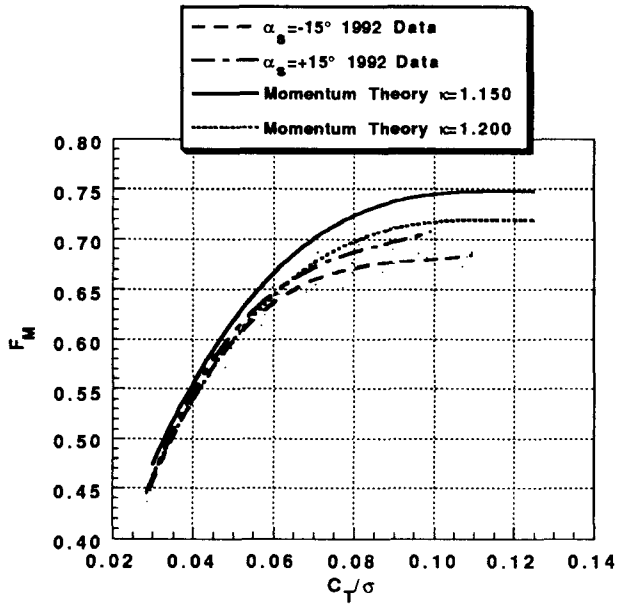

Fig. 9 Effect of rotor shaft angle on figure of merit, M_{TIP}= 0.605

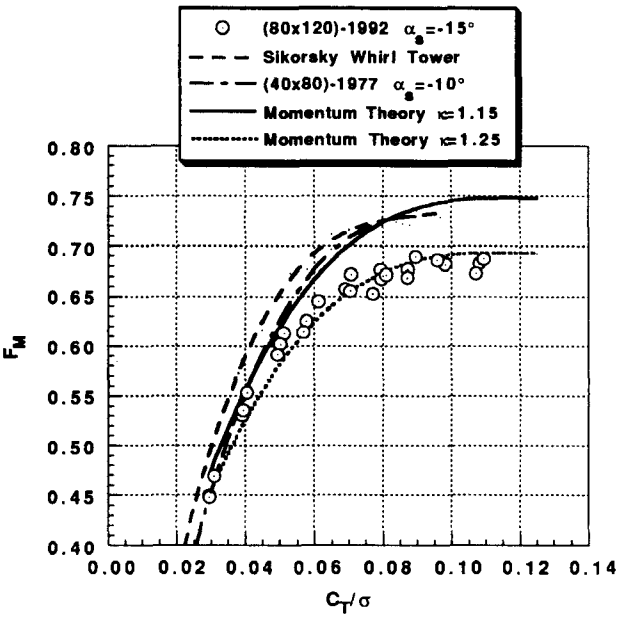

Fig. 11 S-76 rotor hover figure of merit comparison from three different facilities with predictions, M_{TIP}= 0.605

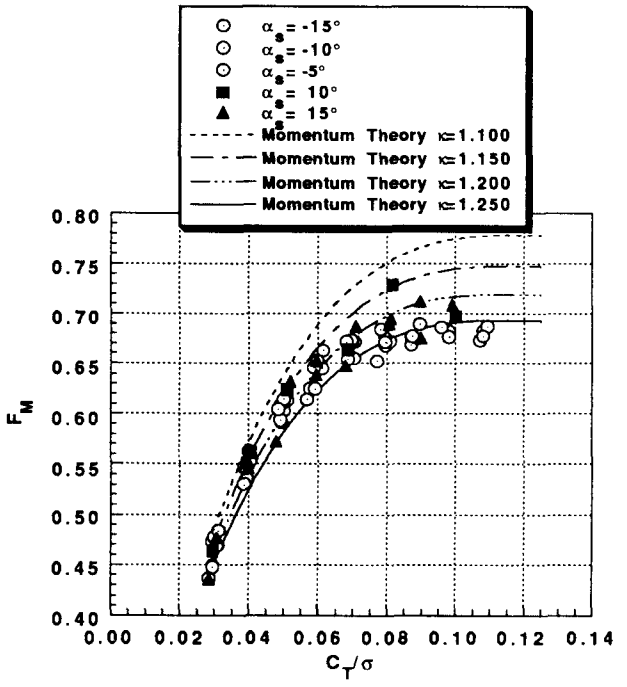

Fig. 10 Comparison of positive α_s with negative α_s effects on rotor figure of merit, M_{TIP}= 0.605.

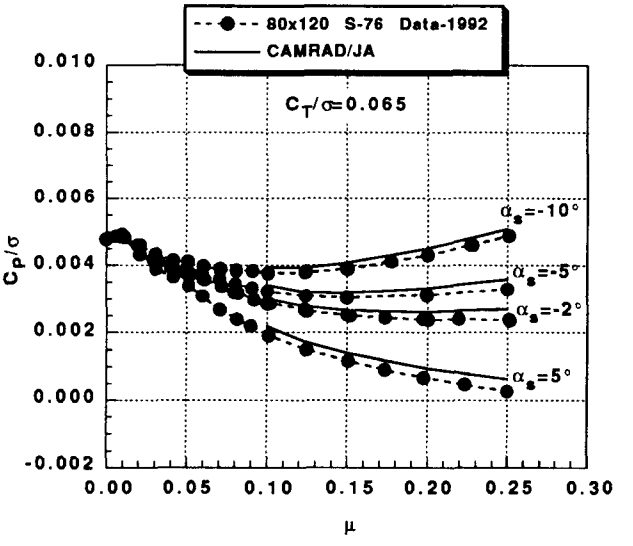

Fig. 12 The effects of advance ratio and α_s on measured and predicted rotor power, C_T/σ= 0.065, M_{TIP}= 0.605.

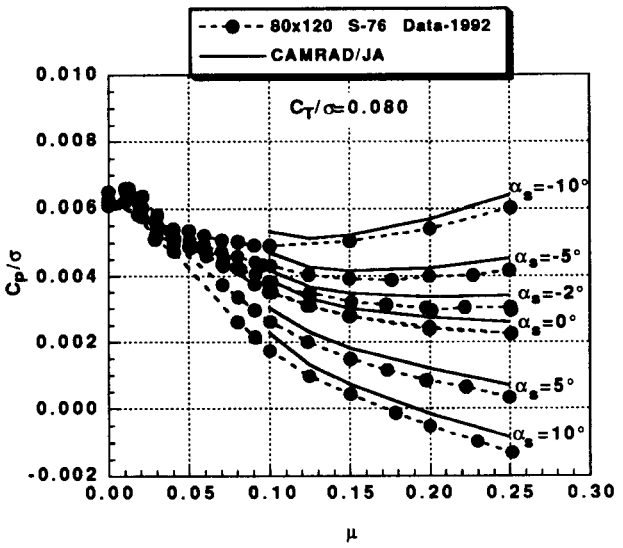

Fig. 13 The effects of advance ratio and α_s on measured and predicted rotor power, C_T/σ= 0.080, M_{TIP}= 0.605.

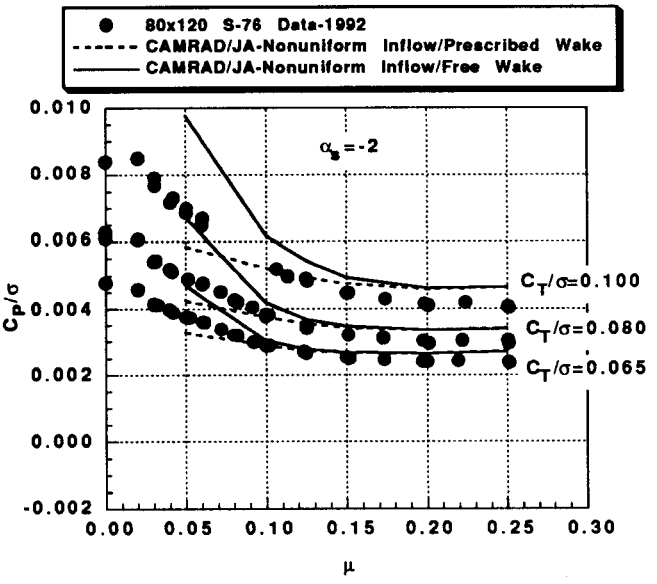

Fig. 15 Comparison of CAMRAD/JA calculations using different wake models with measured rotor power, α_s = -2 deg, C_T/σ= 0.065, 0.080, 0.100, M_{TIP}= 0.605.

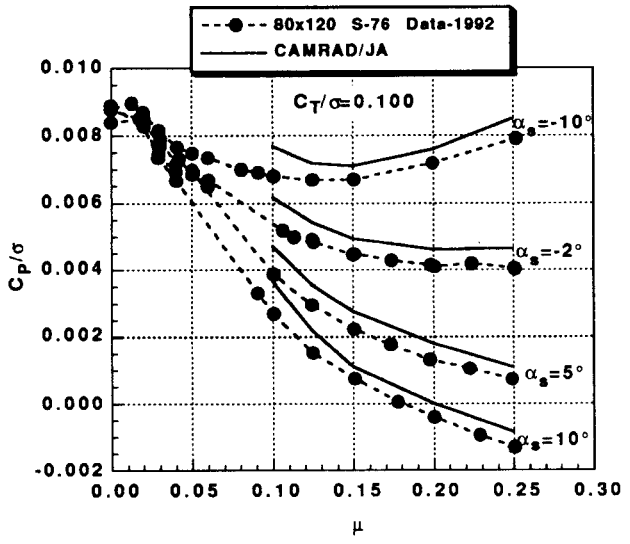

Fig. 14 The effects of advance ratio and α_s on measured and predicted rotor power, C_T/σ= 0.100, M_{TIP}= 0.605.

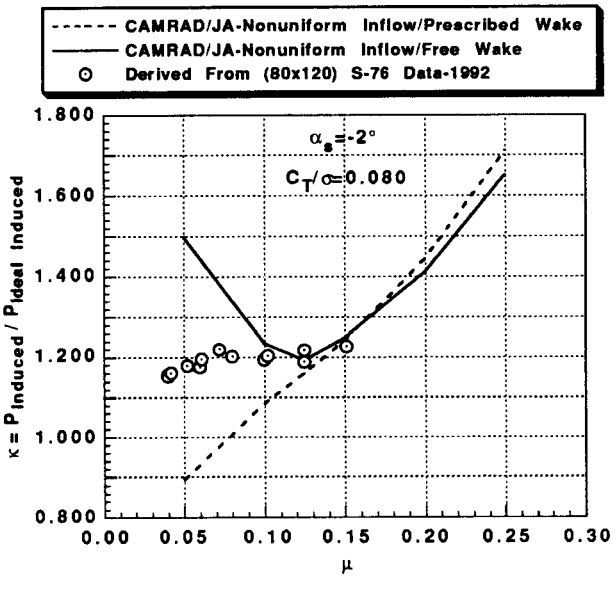

Fig. 16 Rotor κ ratio values derived from data and calculated using CAMRAD/JA prescribed wake and free wake model, α_s = -2 deg, C_T/σ= 0.080, M_{TIP}= 0.605.

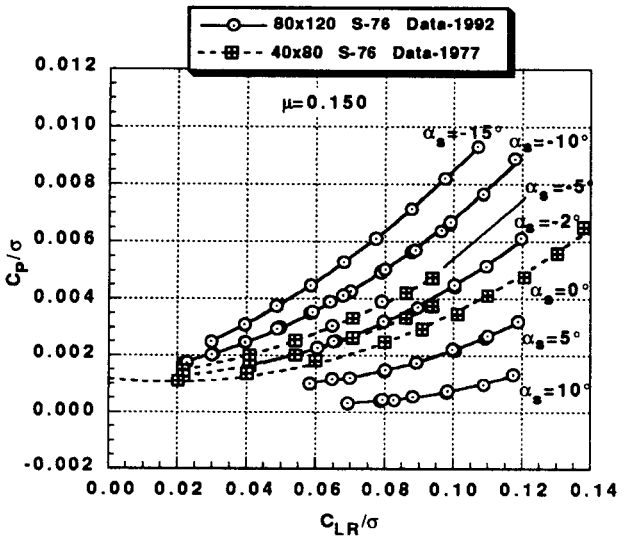

Fig. 17 Rotor power vs rotor lift data from 40x80 data and 80x120 tests for various rotor shaft angles at an advance ratio of 0.15, M_{TIP}= 0.605.

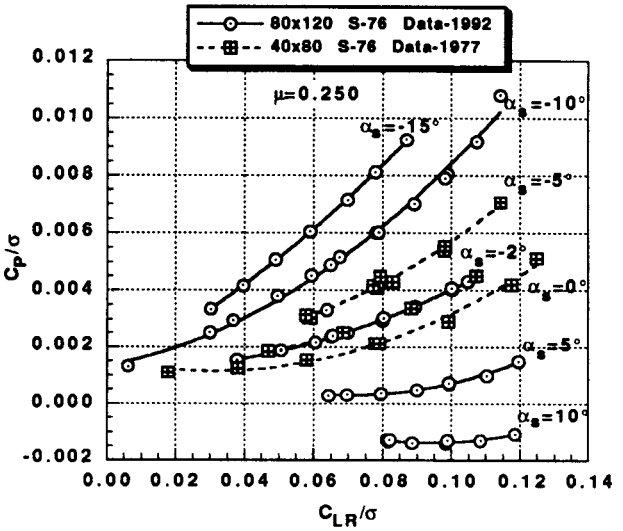

Fig. 19 Rotor power vs rotor lift data from 40x80 data and 80x120 tests for various rotor shaft angles at an advance ratio of 0.25, M_{TIP}= 0.605.

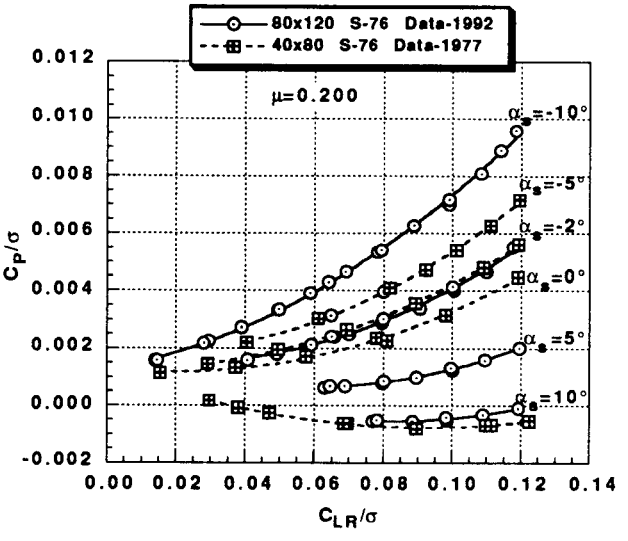

Fig. 18 Rotor power vs rotor lift data from 40x80 data and 80x120 tests for various rotor shaft angles at an advance ratio of 0.20, M_{TIP}= 0.605.

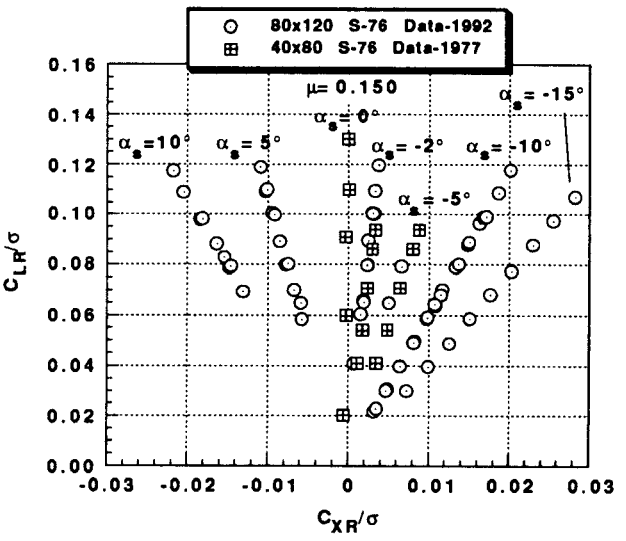

Fig. 20 Propulsive force vs rotor lift data from 40x80 data and 80x120 tests for various rotor shaft angles at an advance ratio of 0.15, M_{TIP}= 0.605.

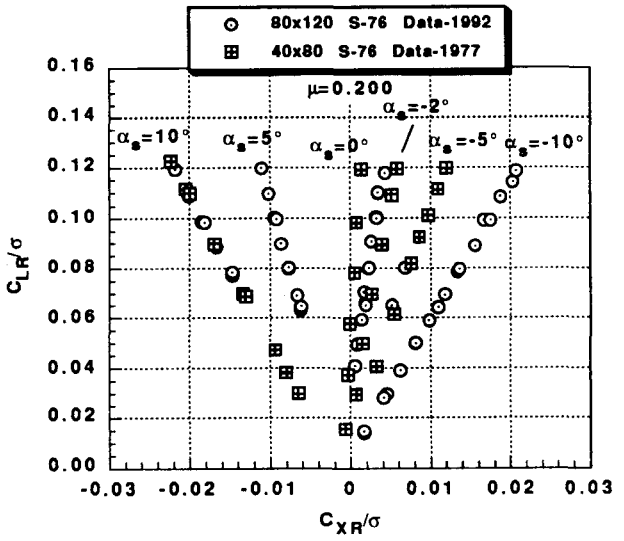

Fig. 21 Propulsive force vs rotor lift data from 40x80 data and 80x120 tests for various rotor shaft angles at an advance ratio of 0.20, M_{TIP}= 0.605.

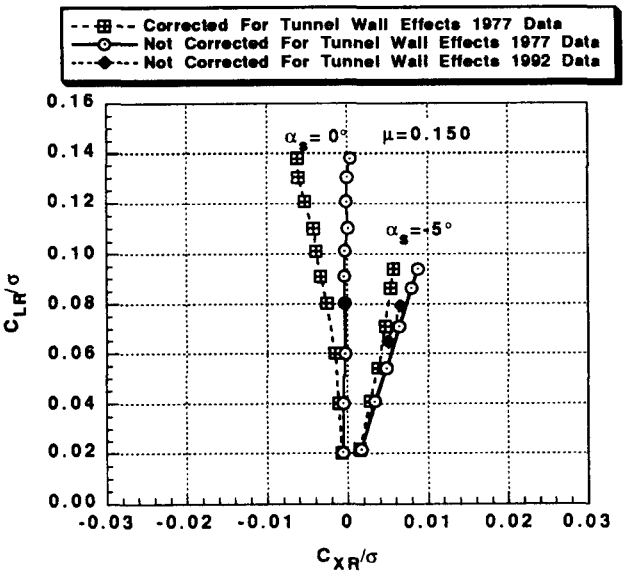

Fig. 23 Rotor propulsive force vs rotor lift data from 40x80 test (with and without wall corrections) and 80x 120 test (without wall corrections) at an advance ratio of 0.15, M_{TIP}= 0.605.

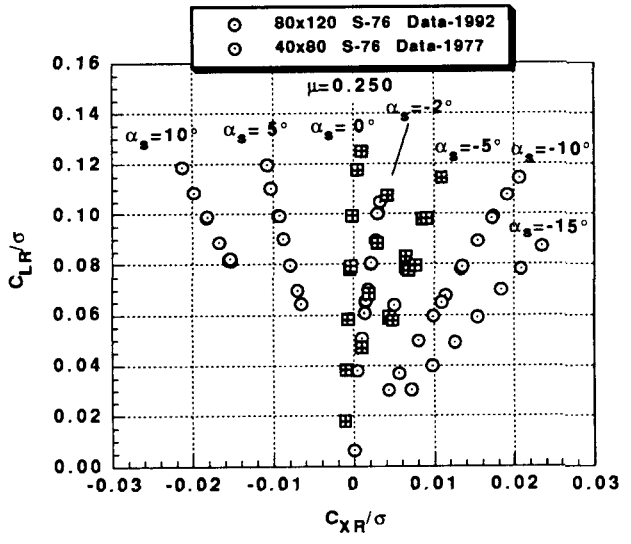

Fig. 22 Propulsive force vs rotor lift data from 40x80 data and 80x120 tests for various rotor shaft angles at an advance ratio of 0.25, M_{TIP}= 0.605.

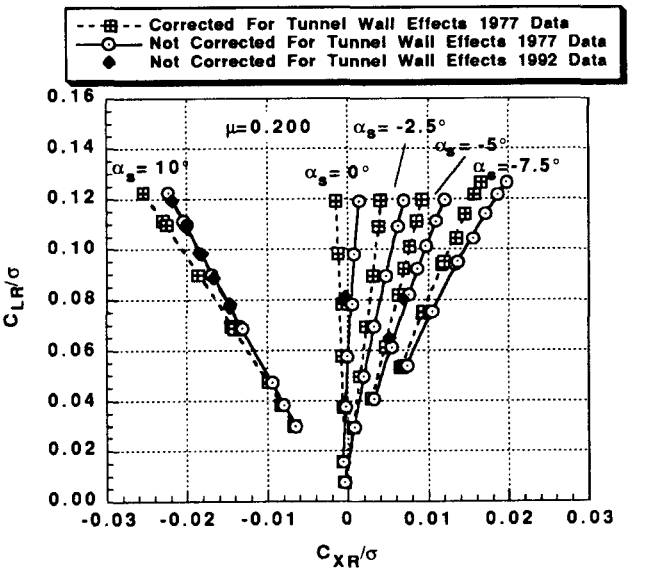

Fig. 24 Rotor propulsive force vs rotor lift data from 40x80 test (with and without wall corrections) and 80x 120 test (without wall corrections) at an advance ratio of 0.20, M_{TIP}= 0.605.

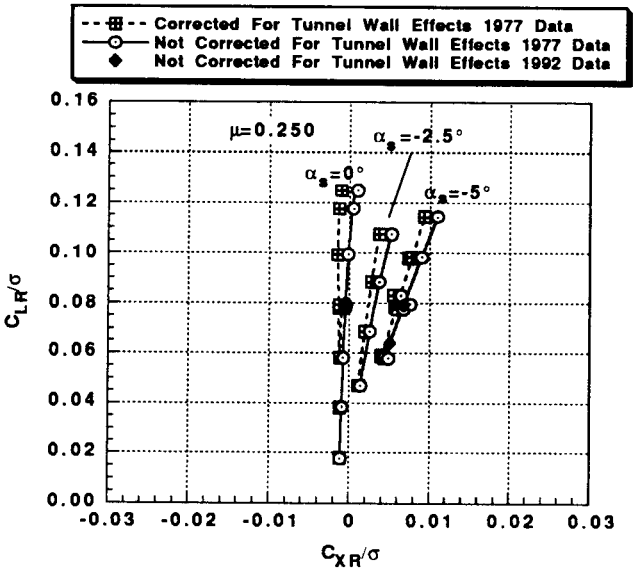

Fig. 25 Rotor propulsive force vs rotor lift data from 40x80 test (with and without wall corrections) and 80x 120 test (without wall corrections) at an advance ratio of 0.25, M_{TIP}= 0.605.

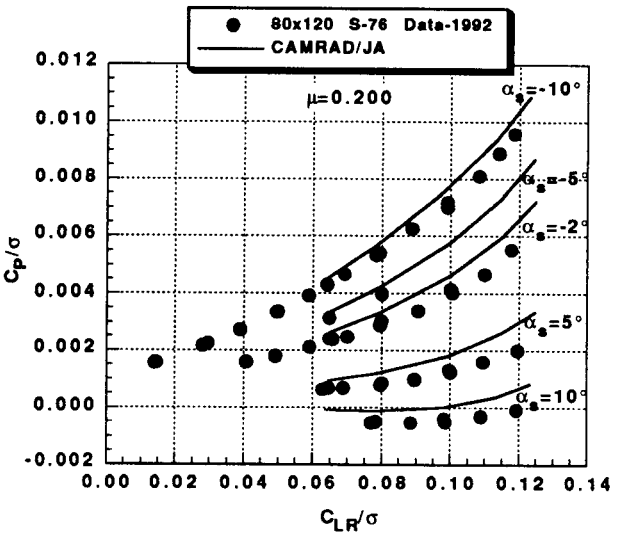

Fig. 27 Measured and calculated rotor power vs rotor lift for various rotor shaft angles at an advance ratio of 0.20, M_{TIP}= 0.605.

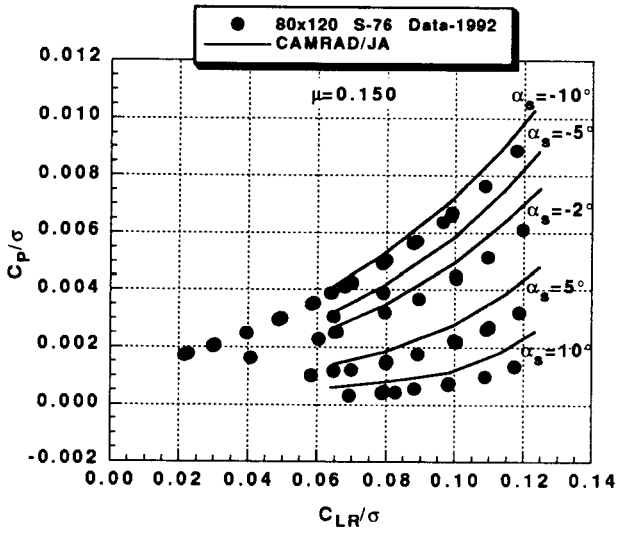

Fig. 26 Measured and calculated rotor power vs rotor lift for various rotor shaft angles at an advance ratio of 0.15, M_{TIP}= 0.605.

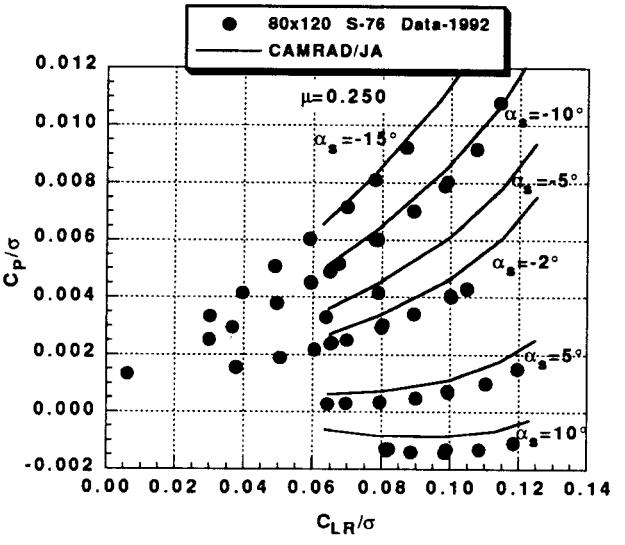

Fig. 28 Measured and calculated rotor power vs rotor lift for various rotor shaft angles at an advance ratio of 0.25, M_{TIP}= 0.605.

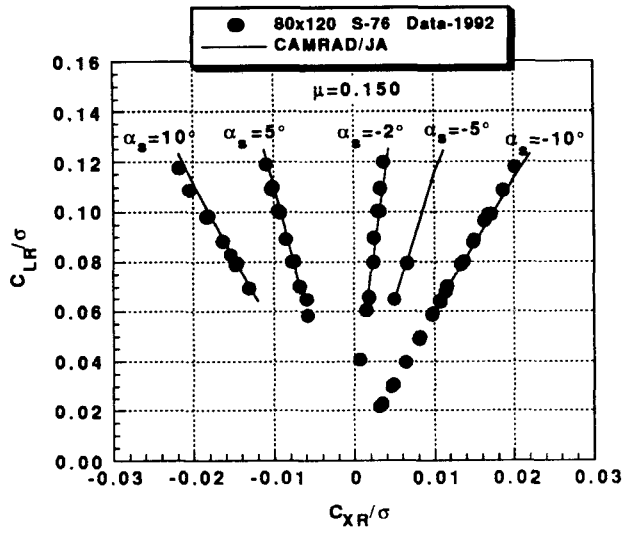

Fig. 29 Measured and calculated rotor propulsive force vs rotor lift for various rotor shaft angles at an advance ratio of 0.15, M_{TIP}= 0.605.

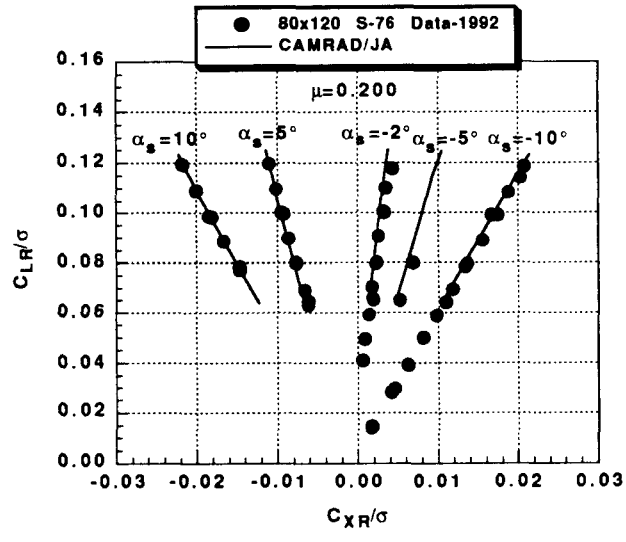

Fig. 30 Measured and calculated rotor propulsive force vs rotor lift for various rotor shaft angles at an advance ratio of 0.20, M_{TIP}= 0.605.

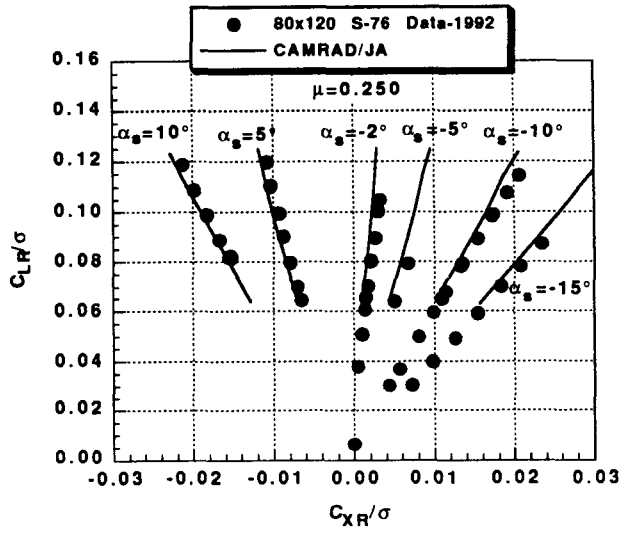

Fig. 31 Measured and calculated rotor propulsive force vs rotor lift for various rotor shaft angles at an advance ratio of 0.25, M_{TIP}= 0.605.